# SECTION 5

# METHODS AND MATERIALS

## APPARATUSES - LABORATORY AND FIELD CONTACTOR UNITS

### Laboratory Contactors

Four downflow, packed-column contactors were used in the laboratory study. Each column contained a different limestone particle size. The column diameters were chosen to yield a column-to-particle diameter ratio of at least ten to minimize the effect of the higher porosity at the wall on the flow through the bed . The four columns and the water feed system are illustrated in Figure 6.

Column A in Figure 6 was constructed of clear acrylic plastic and contained limestone particles with a 0.96 cm mean diameter. The column inside diameter was 15.2 cm and the length was 3.5 m. Columns B, C and D were constructed of polyvinyl chloride pipe. Columns B and C both had inside diameters of 15.2 cm and Column D had an inside diameter of 38.1 cm. The stone sizes (mean diameter) in these columns were 0.54 cm, 1.5 cm, and 3.2 cm for Columns B, C, and D respectively. All three columns were 2.1 m. long.

All four columns in Figure 6 were equipped with through-the-wall sampling tubes. The tubes were spaced in the axial direction at 15.2 cm intervals at the influent end and at 30.4 cm intervals over the remaining portion of each column.

Each sampling tube (0.6 cm diameter acrylic plastic) extended to the center of the column. Five 0.25 cm diameter holes were drilled in the upper part of each tube. Each tube was cemented to a plastic adaptor which was threaded into the column wall. A short length of plastic tubing with a hose clamp was attached to the plastic adaptor. A drawing of a typical sampling tube is included within Figure 6.

The water supply and flow control system used with the four laboratory columns is shown in Figure 6. The raw water was pumped from a 200 L plastic tank to a constant head tank located above Column A. Overflow from the constant head tank returned to the plastic tank. Flow control for each column effluent was accomplished using a flowmeter with a micrometer controlled

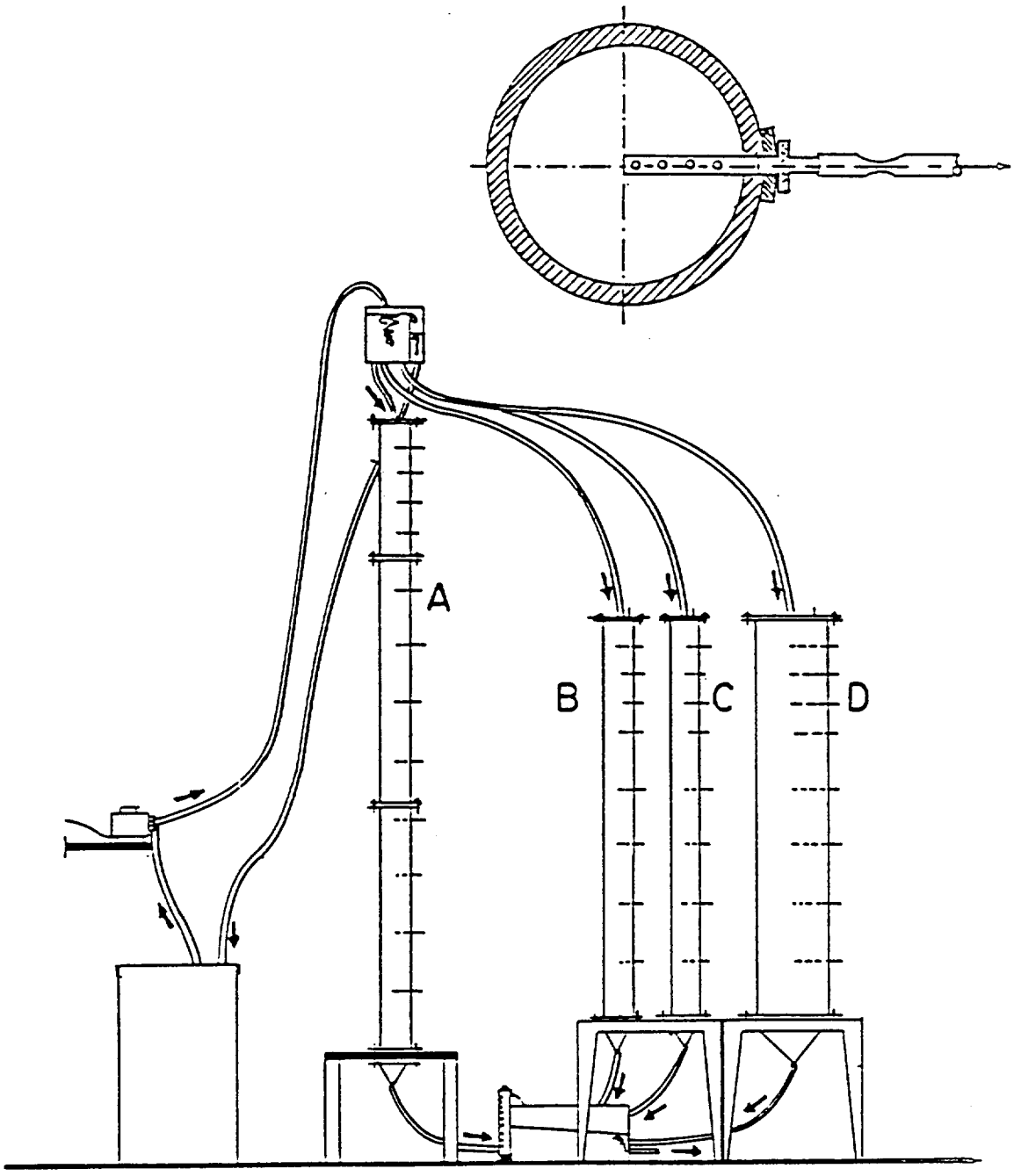


Figure 6. Laboratory columns with water supply and flow control system. Insert is a drawing of a typical through-the-wall sampling tube.

valve assembly. From the flowmeter the water discharged to a small open chamber and from this unit to a floor drain. The flowmeter calibration was checked frequently using a volumetric cylinder and a stopwatch.

The limestone was washed with tap water and placed in each column layer by-layer to facilitate installation of the sampling tubes and to minimize later compaction of the bed. Gentle tapping and shaking of the column were used to consolidate the bed as it was installed.

Field Contactors

Three devices were studied in the field investigation. These included a large baffled-box device which was submerged in a mountainside spring at the head end of a rural resort water supply system and two small column-type units which were used for individual resort cabins. One of these small units was obtained from Culligan, Inc.*

The baffled-box contactor is described in Figure 7. The unit was constructed several years ago at Syracuse University using 1.9 cm thick marine-grade plywood covered with 2 mm thick plexiglass sheets. The overall dimensions are 0.6 x 0.6 x 1.2 m. Sampling cells which also serve as baffles to direct the flow along the bottom of the chambers were constructed of 0.6 and 1.3 cm plexiglass (each is 12.7 cm x 12.7 cm x 0.6 m). The sides and lid were braced with fiberglass resin coated aluminum angles. Fiberglass resin was also used to coat small areas of the contactor not covered by plexiglass sheets. The unit contained approximately 479 Kg. of 0.96 cm mean diameter limestone particles and the length of the flow path through the limestone was approximately 354 cm. The cross-sectional area perpendicular to the direction of flow was approximately 915 $cm^2$.

The two smaller column type units used in the field study are shown in Figure 8. Column 1 had an inside diameter of 20.2 cm and an overall length of 130 cm. Flow entered this column at the top, passed down through the bed and exited through a cylindrical plastic strainer connected to a 2 cm, inside diameter plastic pipe which passed up through the center of the bed. Column 1 was constructed of wound fiberglass and contained 60 Kg of crushed limestone (0.96 mean diameter particle size). The overall depth of limestone was 122 cm. Column 1 was a slightly modified version of a container used in ion exchange systems.

*Mention of trade names or commercial products does not constitute endorsement or recommendation for use.

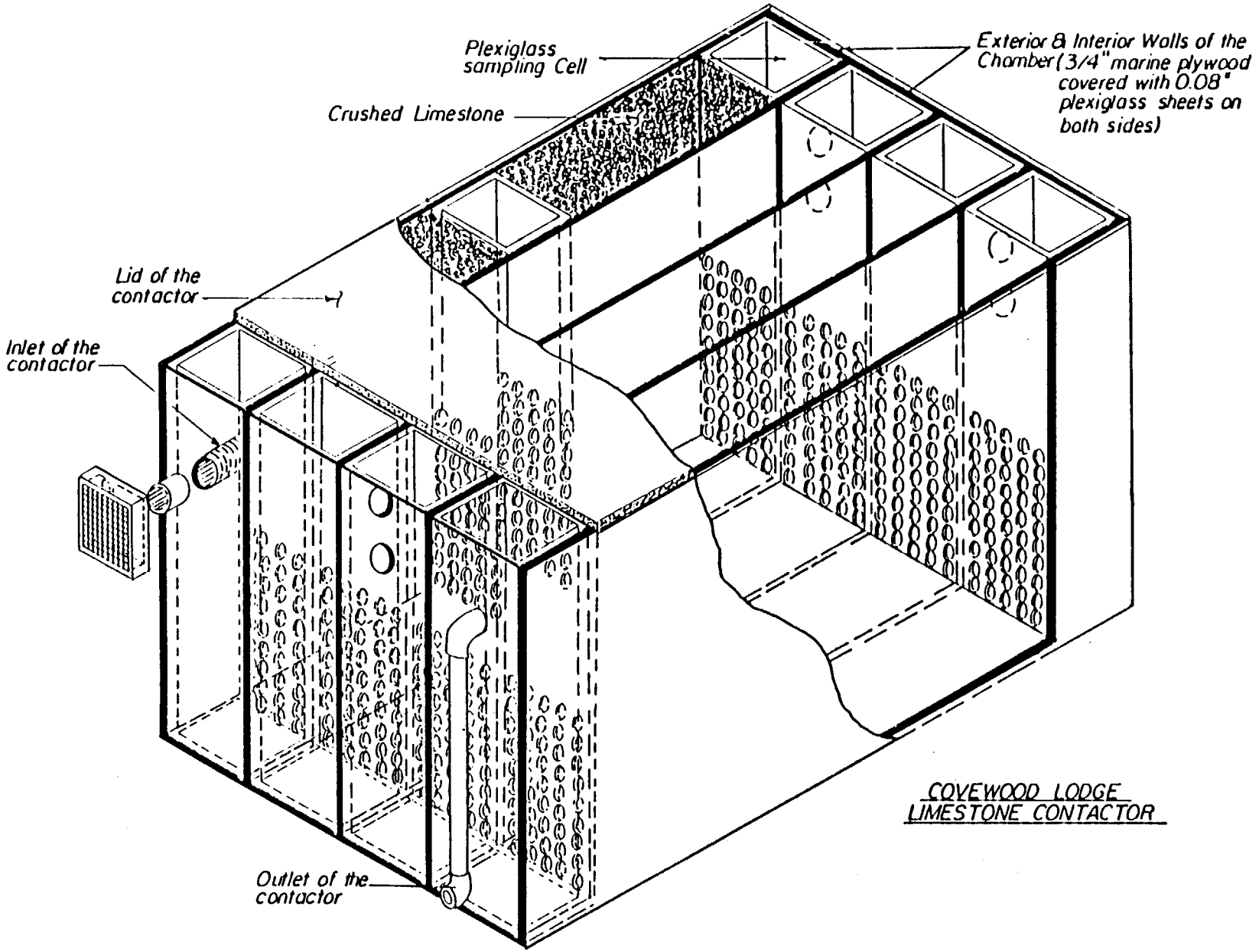


Figure 7. Baffled-box contactor used in the field study. Entire unit was submerged in a mountain-side spring.

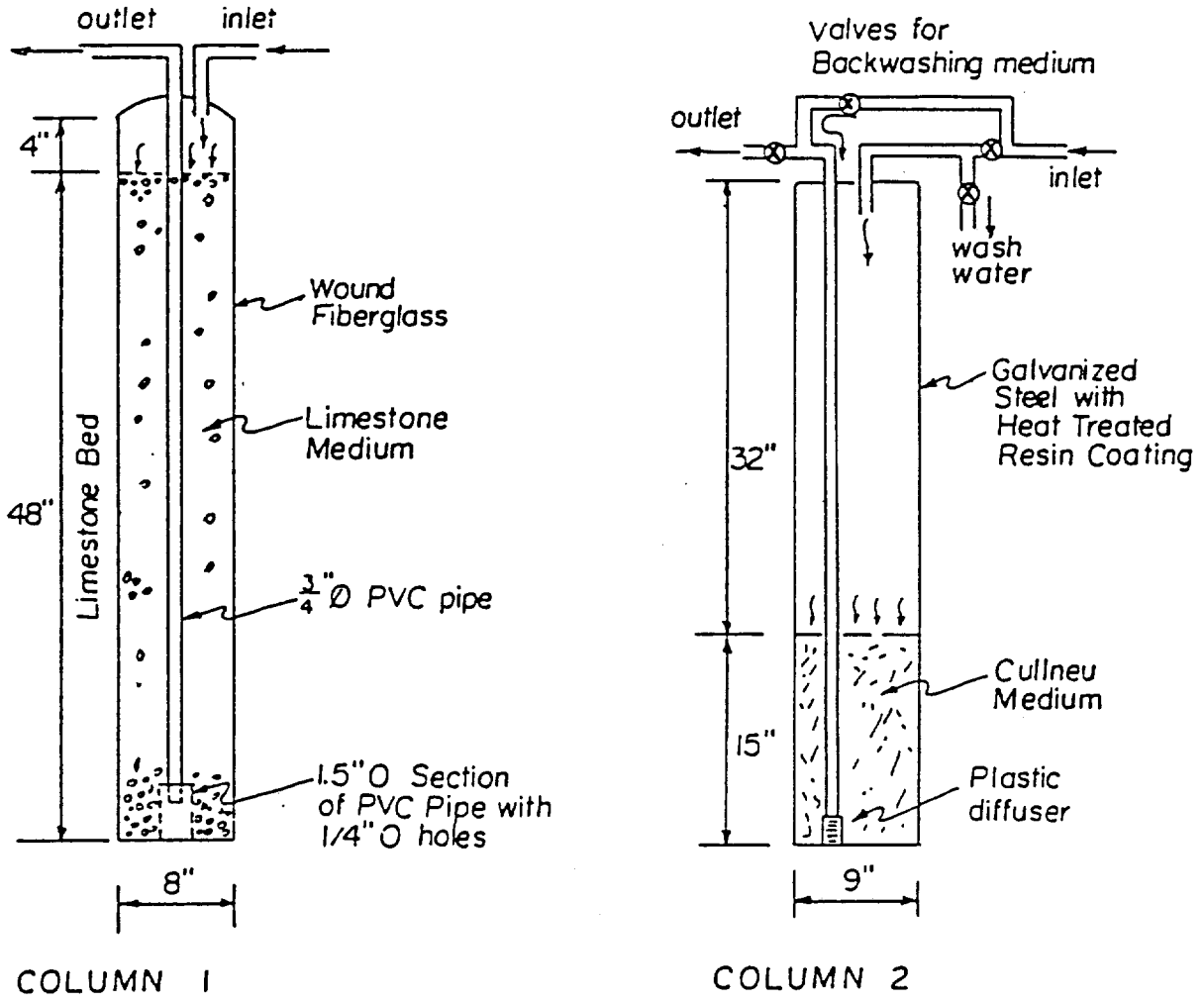


Figure 8. Wound-fiberglass and Culligan contactors used in the field study. The wound-fiberglass contactor was filled with limestone and the Culligan unit contained Cullneu, a form of $CaCO_3$ sold by Culligan, Inc. The wound-fiberglass unit was installed in Bayside cottage and the Culligan unit in Henry Covey cottage. (See Figure 9)

Column 2 illustrated in Figure 8, was rented from Culligan, Inc. It had an inside diameter of 23 cm and a total length of 127 cm. It was constructed of galvanized steel coated with a heat treated epoxy resin.

A granular, calcium carbonate medium (Cullneu®, neutralizing medium, catalog number 1600-10) sold by Culligan, Inc.* was used in place of limestone in Column 2. The column was filled to a depth of 40 cm with Cullneu®. The flow conditions within Column 2 were very similar to those in Column 1, however, Column 2 was equipped with a valve arrangement at the top which allowed one to direct water into the effluent pipe to backwash the medium by upflow through the bed.

The baffled-box contactor and the two column units were installed at the Covewood Lodge, a resort with housekeeping cottages and a rustic lodge located in the Adirondack Region of New York State near Old Forge. A map illustrating the layout of the gravity-fed supply system is presented in Figure 9. The baffled-box contactor was installed, completely submerged, in the spring which serves the seven cottages on the west side of the resort. The spring water elevation was approximately fifteen meters above the ground floors of the cottages. Water flowed for a distance of approximately 20 ft. (6 m) into two, 400 gallon, (1600 L) galvanized steel storage tanks. Flow to the cottages from the storage tanks was through a 3.8 cm diameter plastic pipe. The plumbing in each cottage was copper pipe soldered with 50/50 lead-tin solder. The installation of the baffled-box contactor installed within the spring is illustrated in Figure 10. Bay Side and Hillside cottages contained approximately 30 m (100 ft) and 15 m (50 ft) of 1.3 cm (½ in.) diameter copper pipe, respectively with approximately forty 50/50 lead-tin solder joints per cottage or two joints per meter of copper pipe.

The wound fiberglass column with limestone particles (Column 1, Figure 8) was installed in the heated basement of Bay Side cottage (see Figure 9). The unit was used during the months of January, February, March and April 1984 when the plastic line from the spring and baffled-box contactor became frozen and it was necessary for the resort owner to supply water to the winterized cottages by pumping water directly from Big Moose Lake. The contactor in Bay Side Cottage was installed on the pressure side of a pressure switch activated supply pump. The cottage contains two small living units, each

*Mention of trade names or commercial products does not constitute endorsement or recommendation for use.

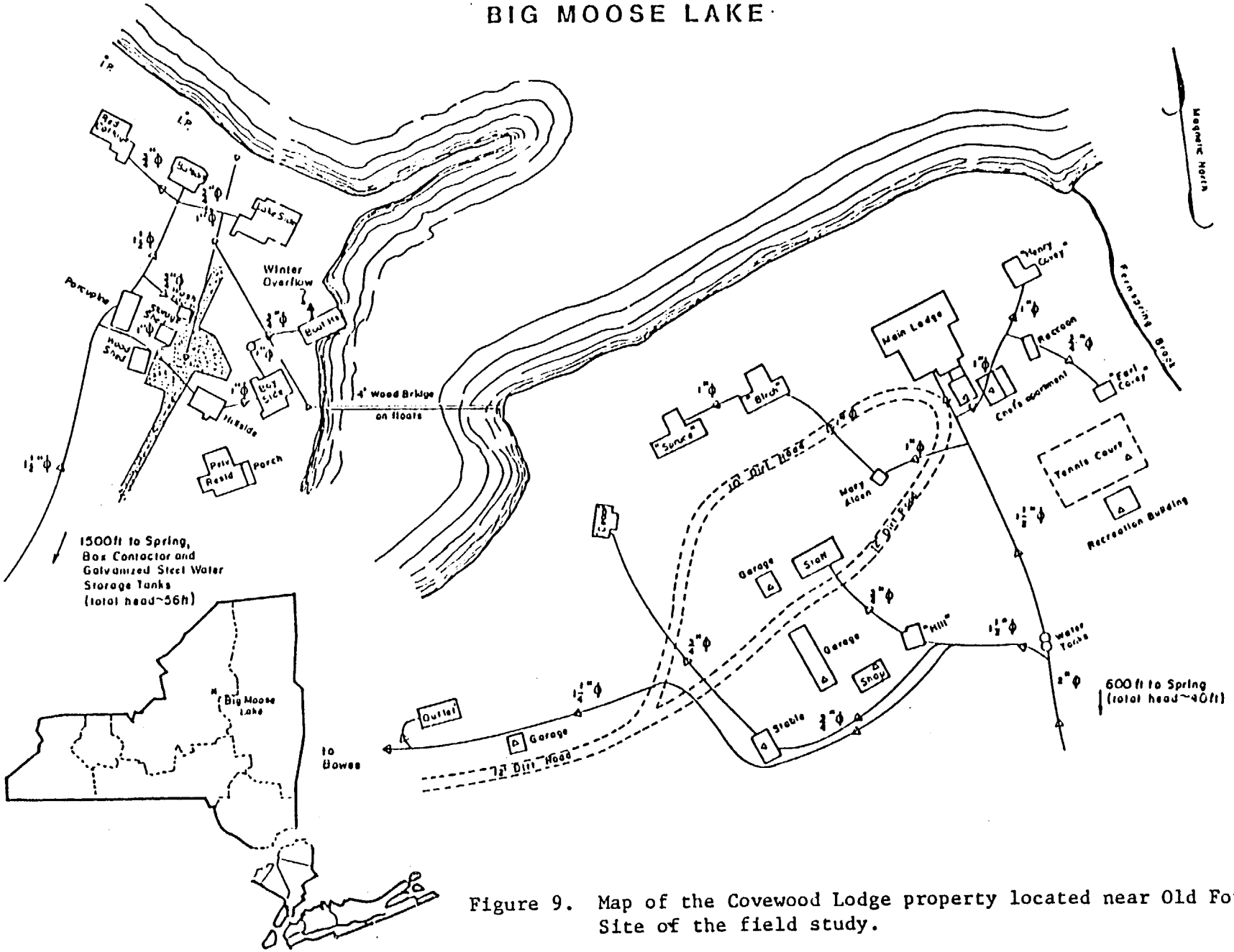


Figure 9. Map of the Covewood Lodge property located near Old Forge, NY. Site of the field study.

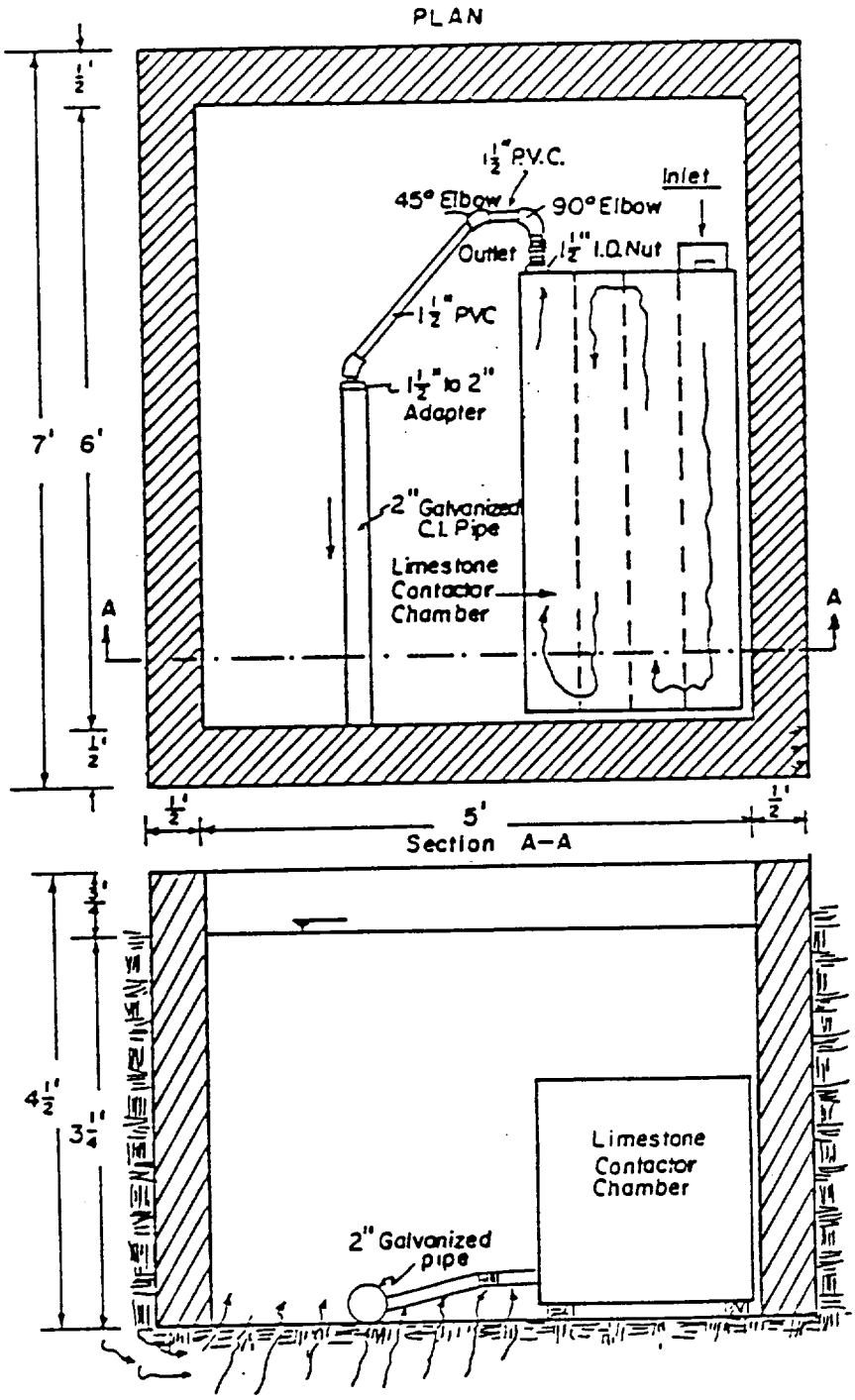


Figure 10. Diagram showing the installation of the baffled-box contactor in the spring at Covewood.

has a kitchen and a bathroom with a toilet, sink and shower. Normal total occupancy during the winter (most but not all guests limit their stay to a weekend) is four adults.

The Culligan column with Cullneu® medium was installed in the basement of a cottage (Henry Covey, Figure 9) on the east side of the resort. The east side of the resort receives water from a spring, which at the time of this study, contained a marginally effective limestone contactor installed by the resort owner. The unit in this spring was somewhat ineffective because of significant short-circuiting. The Henry Covey cottage is winterized and has a kitchen and a bathroom with sink, toilet and shower. Normal occupancy is two persons.

Estimates of limestone contactor cost are given in Appendix C.

## Limestone Characteristics

The limestone used throughout the study was obtained from a quarry in Boonville, New York. The limestone was analyzed in the laboratory to determine its physical and chemical characteristics.

Chemical Characteristics - A sample of limestone was ground to a powder (particle diameter less than 0.29 mm) and then washed with tap water and dried 24 hours at 105°C.

Three 0.2 gram portions of the powdered limestone were dissolved in 50 ml 1:1 $HCL/HNO_3$. After dilution with deionized water elemental analysis was conducted by atomic absorption spectrophotometry.

It was determined that the cation content of the Boonville limestone is (by mass) 85 percent calcium, 12.3 percent aluminum and 2.4 percent magnesium. Iron, Mn, Zn, Cu and Cd were present at less than 0.1 percent and Pb, K and Na were not detected. These results indicate that the Boonville limestone is essentially a "high calcium" limestone.

A supplemental experiment was conducted in which a measured quantity of Boonville limestone was dissolved in concentrated hydrochloric acid in a closed system. The $CO_2$ evolved was captured and its amount measured. This result combined with the calcium measurement indicates that the Boonville stone contains 79% $CaCO_3$ by mass. Therefore, although it can be labeled a high calcium stone it is not of high purity.

The effective $CaCO_3$ solubility product for the limestone was determined by placing 0.10 gram samples of the powdered limestone in twelve open flasks containing 100 ml of deionized water. Different amounts of acid were added to each flask (between 0.25 to 1000 μeq/L using 1N HCl) so that the initial pH of the samples was between 3.00 and 6.60. The flasks were agitated on a shaker table in the 20°C room for one week. At the end of the equilibration period samples were filtered using 0.45 μm millipore membrane filter and analyzed to determine Ca, Mg, DIC and pH.

The molar concentrations of these constituents for each sample were input to the MINEQL chemical equilibrium computer program (Westall et al., 1976) using the following conditions:

a - Fixed carbon dioxide partial pressure of $10^{-3.5}$ atm.

b - Fixed pH (measured final value for each sample)

c - Total hydrogen ion concentration equal to the molar concentration of acid initially added to the sample.

A solubility product of $CaCO_3$ for the limestone of each sample was calculated as the product of the equilibrium activities of calcium and carbonate computed by the computer program. The average effective solubility product of $CaCO_3$ in Boonville limestone was found to be $10^{-8.71}$ (20°C). The experimental results and the computed values of the effective solubility product are listed in Table 6.

Physical Characteristics - The four size fractions of limestone particles obtained from the Boonville quarry were analyzed to determine particle size, sphericity and mass density.

The median particle size for each size fraction was determined using a standard ASTM (ASTM Manual 447-4) sieve analysis. The percent by weight finer than a given sieve opening was plotted as a function of the size of the sieve opening on arithmetic probability graph paper. The median particle size was determined by interpolation from this graph. In the case of the 0.96 cm median size fraction, 90 percent of the particles were between 0.7 and 1.3 cm.

The volume-weighted mean particle diameter was determined by measuring the volume of at least 1200 particles in each size fraction. Particle volume

Table 6 Effective Solubility of Crushed Limestone
Experimental Results

| Sample Number | Acidity Added eq/l HCl | Initial pH pHo | Final pH pHf | Final DIC mgC/L | Final Calcium Conc. mgCa/L | Final Mag. Conc. mgMg/L | Computed pKsp |
|---|---|---|---|---|---|---|---|
| 1 | 0.25 | 6.6 | 7.54 | 11.9 | 23.08 | 0.18 | 9.663 |
| 2 | 20 | 4.7 | 7.85 | 12.38 | 23.87 | 0.18 | 8.998 |
| 3 | 60 | 4.22 | 7.88 | 12.38 | 25.61 | 0.2 | 8.94 |
| 4 | 100 | 4.0 | 7.92 | 12.38 | 24.41 | 0.18 | 8.881 |
| 5 | 140 | 3.85 | 7.89 | 10.24 | 21.88 | 0.18 | 8.988 |
| 6 | 200 | 3.7 | 7.86 | 10.95 | 24.57 | 0.18 | 8.844 |
| 7 | 260 | 3.59 | 7.92 | 9.29 | 23.7 | 0.19 | 8.894 |
| 8 | 300 | 3.52 | 7.94 | 9.52 | 24.24 | 0.19 | 9.029 |
| 9 | 340 | 3.4 | 8.09 | 10.71 | 28.3 | 0.21 | 8.48 |
| 10 | 400 | 3.4 | 8.11 | 11.43 | 29.95 | 0.21 | 8.416 |
| 11 | 500 | 3.3 | 8.11 | 10.48 | 31.81 | 0.23 | 8.389 |
| 12 | 1000 | 3.0 | 8.02 | 9.29 | 44.4 | 0.33 | 8.422 |

was measured by drying a random sample of particles at 105°C for 24 hours. Each particle in the sample was weighed and numbered and then carefully suspended in a small volumetric cylinder filled with water. The volume displaced was accurately measured with a 1 ml pipet. The volume-weighted mean diameter, $d_p$, for each fraction was calculated using

$$d_p = \left[\frac{6\ V_p}{n\ \pi}\right]^{1/3} \tag{10}$$

where $V_p$ is the total measured volume and n is the number of particles included in the measurement. In the case of the size fraction with a 1.01 cm median diameter (sieve analysis) the volume weighted mean diameter was 0.93 cm. The results of the particle size measurements for the four fractions are given in Table 7. The diameter used for a given fraction in model calculations was the average of the value obtained by the sieve analysis and the value obtained by fluid displacement. The sieve analysis results were approximately normally distributed and therefore it is reaonable to assume that the median size from the sieving/weighing procedure and the mean size from the fluid displacment measurements should be nearly the same since the particles all have the same density.

The sphericity of a particle is equal to the surface area of a sphere with the same volume as the particle divided by the measured surface area of the particle. The sphericity of each particle, $\psi_i$, was determined by

$$\psi i = \frac{(6\ V_i/\pi\ )2/3\ (\ \pi/4)}{A_i} \tag{11}$$

where $V_i$ is the volume of the particle measured by fluid displacment and $A_i$ is the actual surface area measured planimetrically. The sphericity listed in Table 7 for each size fraction is the average value for the particles in the sample. The sample size for each size fraction was approximately fifty particles.

The average sphericity ranged from 0.83 for the 3.20 cm size fraction to 0.78 for the 1.50 cm fraction. In the case of the 0.96 cm fraction the measured sphericities ranged from 0.50 to 0.98, with an average value of 0.79.

TABLE 7 Limestone Particle Size and Sphericity Analysis Results

| Size Fraction | Mean Diameter Sieve Analysis (cm) | Volume Weighted Mean Diameter, dp (cm) | Diameter Used in Design Calculations, d(cm) | Particle Sphericity (dimensionless) |
|---|---|---|---|---|
| I | 3.20 | ---- | 3.20 | 0.83 |
| II | 1.45 | 1.55 | 1.50 | 0.78 |
| III | 1.01 | 0.93 | 0.97 | 0.79 |
| IV | 0.55 | 0.54 | 0.54 | 0.81 |

The mean density of the particles was determined by dividing the sum of the particle weights by the sum of their measured volumes. The calculated density was 2.64 $g/cm^3$.

Cullneu is described by the manufacturer, Culligan, Inc., as "a specially graded calcium carbonate compound for neutralizing acid waters which provides consistent dissolving rate for treatment." The particle size is 6-30 mesh or a mean effective diameter of approximately 2.2 mm. The bulk density is approximately 1.5 $g/cm^3$. No other information is available on the Cullneu material.

Limestone Bed Characteristics

A number of tests were conducted to measure pertinent physical characteristics of the packed-bed contactors used in the study. The bed porosity was measured and used with the mean particle diameter and particle sphericity to calculate the area of limestone particle surface per unit volume of interstitial water. This quantity is important in modeling dissolution kinetics. Tracer studies were conducted to measure fluid residence time and axial dispersion in the contactor.

The porosity of a packed bed is the ratio of the void space and the total enclosed volume of the bed. The porosity of each column was determined by measuring the volume of fluid required to displace all the air from the bed. This volume was divided by the total volume of the column to obtain the porosity. The complete procedure was repeated five times.

To evaluate the effect of the column wall on the bed porosity a series of special tests were conducted. Beakers of various sizes and hence various wall plus bottom area to volume ratios were filled with each of four limestone particle sizes and the porosity was measured. The measured porosities have been plotted as a function of the vessel contact area to volume ratio (A/V in $cm^{-1}$) in Figure 11.

The measured porosity for the column which contained the 0.96 cm limestone particles was 0.41 and the vessel contact area to volume ratio was 2.25 $cm^{-1}$. From the least square regression line fitted to the 0.96 cm particle size data points in Figure 11, the expected porosity for a vessel contact area to volume ratio of 0.25 $cm^{-1}$ is 0.43 $\pm$ 0.04. The measured porosity of 0.41

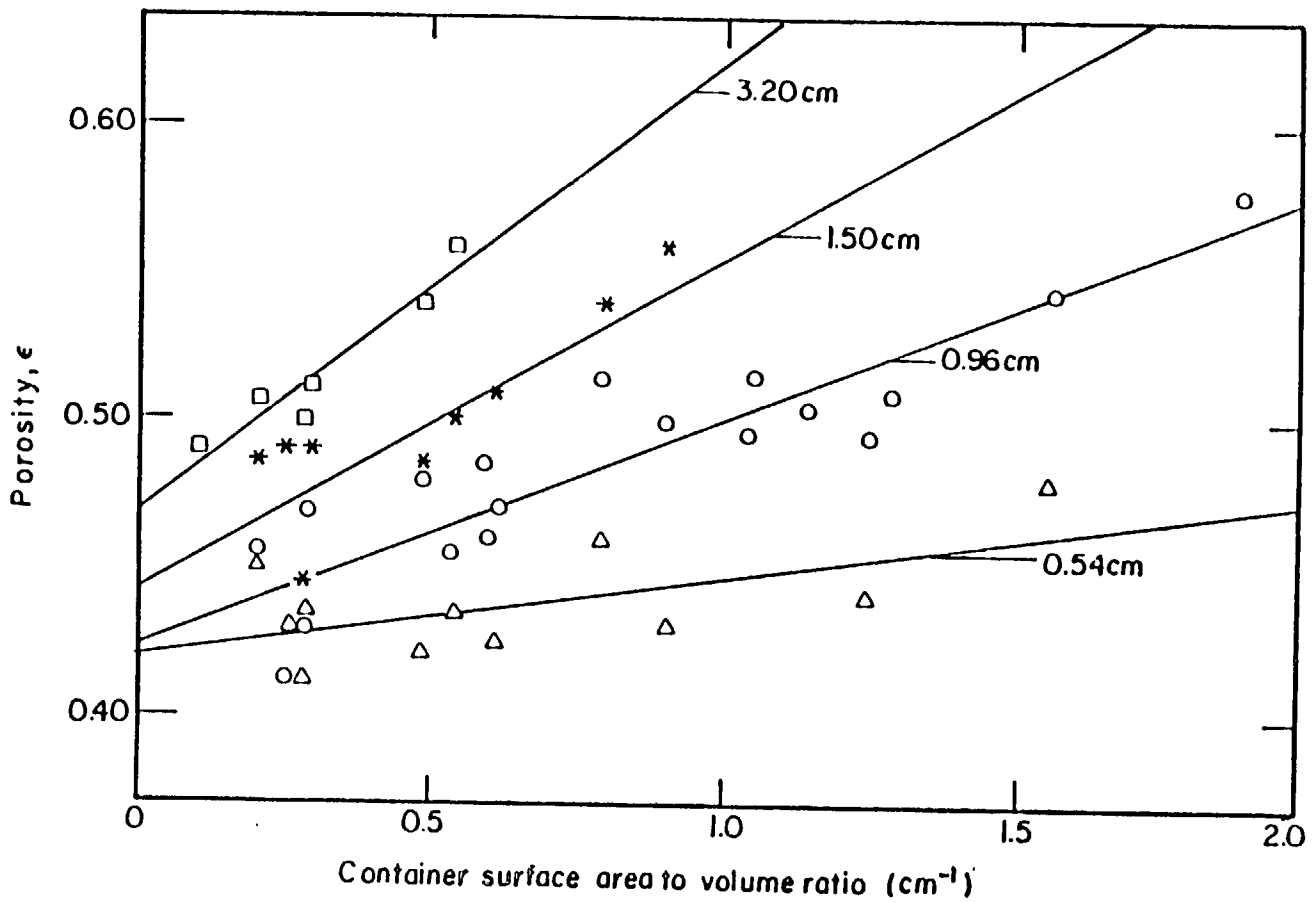


Figure 11. Measured porosity plotted as a function of container surface area to volume ratio for four limestone particle effective diameters. Lines were fitted to the data by the method of least squares.

falls within this range. This result also suggests that under these conditions the column wall has a negligible effect on the overall bed porosity.

The effect of the vessel contact area to volume ratio on the porosity increases with increasing particle size (Figure 11). For example using the four least squares regression lines, for $A/\forall = 1\ cm^{-1}$, the overall porosity is 0.62 for 3.2 cm limestone, 0.55 for 1.5 cm limestone, 0.49 for 0.96 cm limestone and 0.43 for 0.54 cm limestone. The porosities measured (or estimated using Figure 11) for each of the columns used in this study, except the Culligan unit are listed in Table 8.

The limestone particle surface area per unit volume of interstitial water (a, $cm^{-1}$), which was used in modeling the dissolution process, is also listed in Table 8. This quantity was calculated for each column using the measured or estimated porosity ( $\varepsilon$ ) and the measured mean particle size ($\bar{d}$) and sphericity ( $\psi$ ). The equation used is

$$a = \frac{6(1-\varepsilon)}{\bar{d}\ \psi\ \varepsilon} \qquad (12)$$

The contactors described in Figure 6 were used in a set of experiments designed to determine the effect of limestone particle size, flowrate and the depth of the packed-bed on axial dispersion and mean fluid residence time. Axial dispersion may be an important factor in modeling the effect of limestone dissolution on effluent chemistry. Tracer studies were conducted to evaluate axial dispersion and to test calculated values of mean fluid detention time within the bed.

Lithium chloride was used as a tracer salt. Lithium is easily detected (by atomic absorption spectrophotometry), it does not react with nor is it significantly adsorbed by the contents of the columns and the background concentration of lithium was negligible in the tap water used in the tracer experiments.

In most experiments a 200 mg quantity of LiCl dissolved in 10 mL of deionized water (20g Li/L) was injected with a syringe into the feed port at the top of the column. Samples from the effluent port were collected every 15-30 seconds around the peak concentration of the tracer curves and every minute for the remainder of the test. The tracer study was repeated

TABLE 8 Bed porosity and Limestone Particle Surface Area per unit volume of Interstitial Water

| Column | Limestone Particle Diameter, $\bar{d}$ (cm) | Porosity | Limestone Particle Surface Area Per Unit Volume of Interstitial Water, a ($cm^{-1}$) |
|---|---|---|---|
| A, Figure 6 | 0.96 | 0.41 | 11.4 |
| B, Figure 6 | 0.54 | 0.43 | 18.2 |
| C, Figure 6 | 1.50 | 0.49 | 5.3 |
| D, Figure 6 | 3.20 | 0.49 | 2.6 |
| Wound Fiberglass Figure 8 | 0.96 | 0.44* | 9.7 |
| Baffled-Box Figure 8 | 0.96 | 0.44* | 9.7 |

*Estimated Using Figure 11 and measured vessel contact area to volume ratios.
Wound Fiberglass Column, $A/\forall = 0.21\ cm^{-1}$;
Baffled-Box Contactor, $A/\forall = 0.19\ cm^{-1}$.

three times for each flowrate. The results of four experiments are plotted in Figure 12.

The results from each tracer test were analyzed to determine the total mass of lithium injected passing the sampling port using the following equation:

$$[\text{Mass of Lithium Recovered}] = Q \sum_{i=1}^{n} C_i \; t_i \qquad (13)$$

The quantity $\sum_{i=1}^{n} C_i \; t_i$ is the area under the tracer response curve and Q is the volumetric flowrate.

The mean fluid residence time, $\bar{t}$, was determined using the first moment of the tracer response curve, i.e.,

$$\bar{t} = \frac{\Sigma t_i C_i \; \Delta t_i}{\Sigma C_i \; \Delta t_i} \; . \qquad (14)$$

The axial dispersion number was determined by the second moment matching procedure described by Levenspiel and Smith (1957). For low levels of axial dispersion

$$N_D = \frac{\Sigma t_i^2 \; C_i \; \Delta t_i}{2\bar{t}^2 \; \Sigma \; C_i \; \Delta \; t_i} - 0.5 \qquad (15)$$

where $N_D$ is the dimensionless axial dispersion number.

The axial dispersion number and mean fluid residence time were determined for ranges of superficial velocity, limestone particle size and depth of packed-bed. The results obtained are listed in Table 9. Note that the axial dispersion number was less than 0.02 in all cases and therefore the use of Eq. 15 was reasonably appropriate.

A number of investigators including Edwards and Richardson (1968) and Wilhelm (1962) have compiled data from various researchers and noted that for axial dispersion in liquids in packed beds the Peclet number, i.e.,

$$\text{Peclet number} = \frac{\bar{d} \; U_s}{D \; \varepsilon} = \frac{1}{N_D} \cdot \frac{\bar{d}}{L} \; , \qquad (16)$$

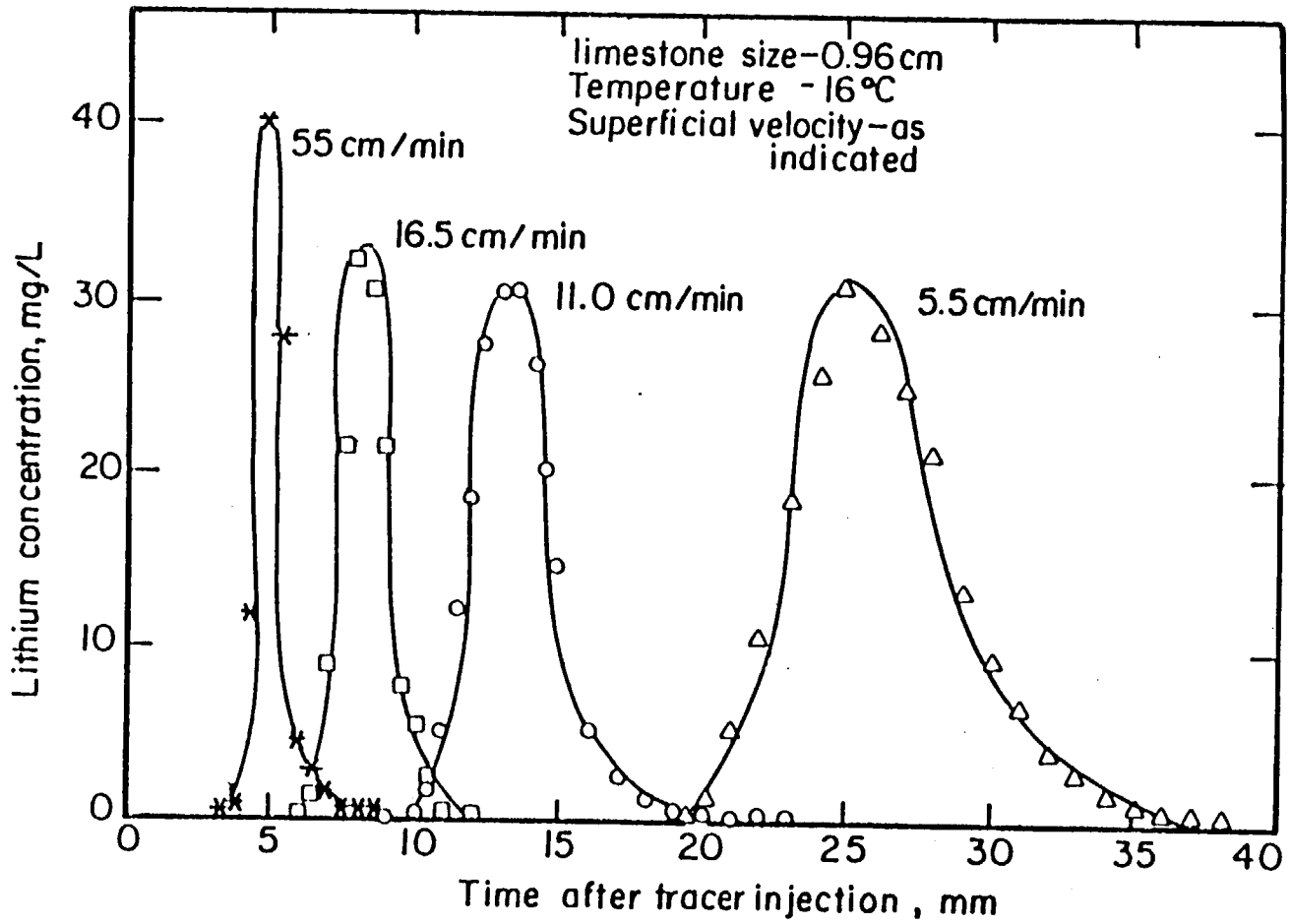


Figure 12. Measured effluent tracer concentration plotted as a function of time elapsed after tracer injection for four values of the superficial velocity. Results were obtained using Column A, Figure 6.

TABLE 9 RESULTS OF TRACER RESPONSE MEASUREMENTS OBTAINED USING LABORATORY COLUMNS (FIGURE 6)

| Exp. No. | Depth L, cm | Particle Size $\bar{d}$, cm | Porosity $\epsilon$ | Superficial Velocity $U_s$, cm/min | Observations: Dispersion Number, $N_D$ | Peclet Number, Pe | Mean Residence Time, $\bar{t}$, min | Tracer Mass Recovered % |
|---|---|---|---|---|---|---|---|---|
| 1 | 305 | 0.96 | 0.41 | 12.2 | 0.0181 | 0.17 | 12.5 | 98 |
| 2 | 152. | 0.96 | 0.41 | 18.2 | 0.0075 | 0.84 | 4.0 | 96 |
| 3 | 335 | 0.96 | 0.41 | 18.2 | 0.0034 | 0.84 | 8.6 | 99 |
| 4 | 335 | 0.96 | 0.41 | 6.1 | 0.0078 | 0.37 | 26.6 | 104 |
| 5 | 335 | 0.96 | 0.41 | 6.1 | 0.0062 | 0.46 | 26.7 | 105 |
| 6 | 335 | 0.96 | 0.41 | 14.7 | 0.0106 | 0.27 | 14.3 | 113 |
| 7 | 335 | 0.96 | 0.41 | 22.0 | 0.0046 | 0.62 | 8.8 | 96 |
| 8 | 335 | 0.96 | 0.41 | 22.0 | 0.0034 | 0.84 | 8.6 | 99 |
| 9 | 335 | 0.96 | 0.41 | 22.0 | 0.0069 | 0.42 | 8.0 | 99 |
| 10 | 335 | 0.96 | 0.41 | 29.3 | 0.0040 | 0.72 | 7.4 | 102 |
| 11 | 335 | 0.96 | 0.41 | 29.3 | 0.0043 | 0.67 | 6.9 | 127 |
| 12 | 335 | 0.96 | 0.41 | 29.3 | 0.0065 | 0.44 | 7.2 | 106 |
| 13 | 335 | 0.94 | 0.41 | 37.5 | 0.0118 | 0.24 | 5.6 | 115 |
| 14 | 335 | 0.96 | 0.41 | 36.7 | 0.0072 | 0.40 | 5.7 | 103 |
| 15 | 335 | 0.96 | 0.41 | 36.7 | 0.0045 | 0.64 | 5.3 | 104 |
| 16 | 335 | 0.96 | 0.41 | 5.4 | 0.0088 | 0.33 | 25.9 | 104 |
| 17 | 335 | 0.96 | 0.41 | 21.4 | 0.0063 | 0.45 | 6.8 | 108 |
| 18 | 335 | 0.96 | 0.41 | 37.5 | 0.0051 | 0.56 | 3.5 | 97 |
| 19 | 335 | 0.96 | 0.41 | 53.5 | 0.0047 | 0.61 | 3.0 | 109 |
| 20 | 61 | 0.54 | 0.43 | 5.4 | 0.0183 | 0.48 | 4.2 | 119 |
| 21 | 152 | 0.54 | 0.43 | 5.4 | 0.0079 | 0.45 | 12.0 | 79 |
| 22 | 213 | 0.54 | 0.43 | 5.4 | 0.0085 | 0.30 | 21.1 | 102 |
| 23 | 213 | 0.54 | 0.43 | 21.5 | 0.0127 | 0.20 | 3.3 | 81 |
| 24 | 213 | 0.54 | 0.43 | 32.2 | 0.0085 | 0.30 | 3.4 | 114 |
| 25 | 213 | 0.54 | 0.43 | 53.7 | 0.0065 | 0.39 | 2.2 | 97 |
| 26 | 213 | 1.50 | 0.49 | 5.3 | 0.0149 | 0.47 | 34.0 | 108 |
| 27 | 213 | 1.50 | 0.49 | 16.0 | 0.0183 | 0.38 | 4.4 | 96 |
| 28 | 213 | 1.50 | 0.49 | 37.4 | 0.0089 | 0.79 | 3.4 | 110 |
| 29 | 213 | 1.50 | 0.49 | 48.1 | 0.0082 | 0.86 | 2.6 | 108 |
| 30 | 213 | 3.20 | 0.49 | 0.3 | 0.0200 | 0.75 | 111.7 | 109 |
| 31 | 213 | 3.20 | 0.49 | 1.1 | 0.0125 | 0.20 | 33.3 | 88 |
| 32 | 213 | 3.20 | 0.49 | 1.9 | 0.0096 | 1.56 | 16.7 | 76 |
| 33 | 213 | 3.20 | 0.49 | 2.7 | 0.0073 | 2.05 | 13.1 | 69 |

is essentially a constant over a wide range of Reynolds numbers and in addition, is only slightly affected by variation in the size of the packing material. For the Reynolds number range of this study ($1 < Re < 100$) all the literature values of the Peclet number analyzed by Wilhelm (1962) and Edwards and Richardson (1968) fall in the interval 0.2 to 2. The range of Peclet numbers for the results listed in Table 7 fall in the range 0.2 to 2 and are therefore consistent with published values.

The mean and standard deviation of the Peclet numbers derived from the quantities listed in Table 7 are 0.50 and 0.21, respectively. These values suggest that a reasonable estimate of the dispersion number for the range of conditions used in this study can be obtained from the following expression,

$$\bar{N}_D = (\overline{Pe})^{-1}(\bar{d}/L) = 2.0\ (\bar{d}/L) \qquad (17)$$

where, $\overline{Pe}$, is the mean value of the Peclet number. Given the standard deviation of 0.21 and the expected value of 2.0, $\bar{N}_D$, should fall in the interval $1.4\ (\bar{d}/L)$ to $3.3\ (\bar{d}/L)$.

The mean fluid residence time in the columns was calculated using the measured bed porosity, $\varepsilon$, (Table 8), the depth of the packed-bed, L, superficial velocity, $U_s$, and the relationship

$$\bar{t}_c = \frac{L\varepsilon}{U_s} \qquad (18)$$

The mean fluid residence time determined using the tracer response curve, $\bar{t}$, plotted as a function of the value calculated using Eq. 18 is given in Figure 13. The agreement obtained is reasonable, a result which tends to support the method used to measure bed porosity and the quality of the tracer response data.

Before it was installed in the field the baffled-box contactor was subjected to a pulse input, lithium chloride tracer response test. The results of this test are plotted in Figure 14.

According to the dimensions of the contactor, the porosity of the bed and the flowrate used in the test (13.6 L/min) the mean residence time should

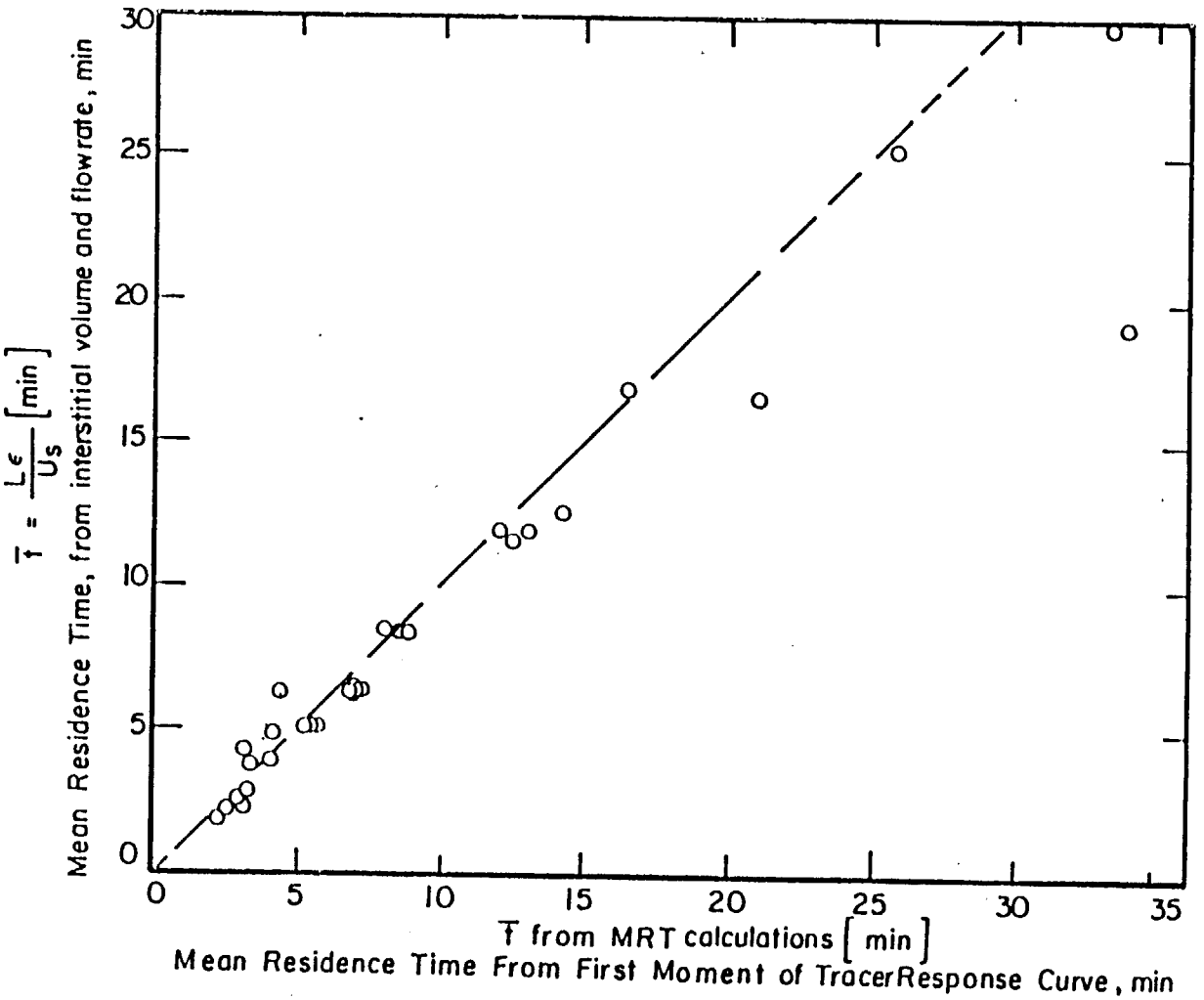


Figure 13. Mean residence time calculated using the superficial velocity and measured porosity plotted as a function of the mean residence time from the tracer experiments.

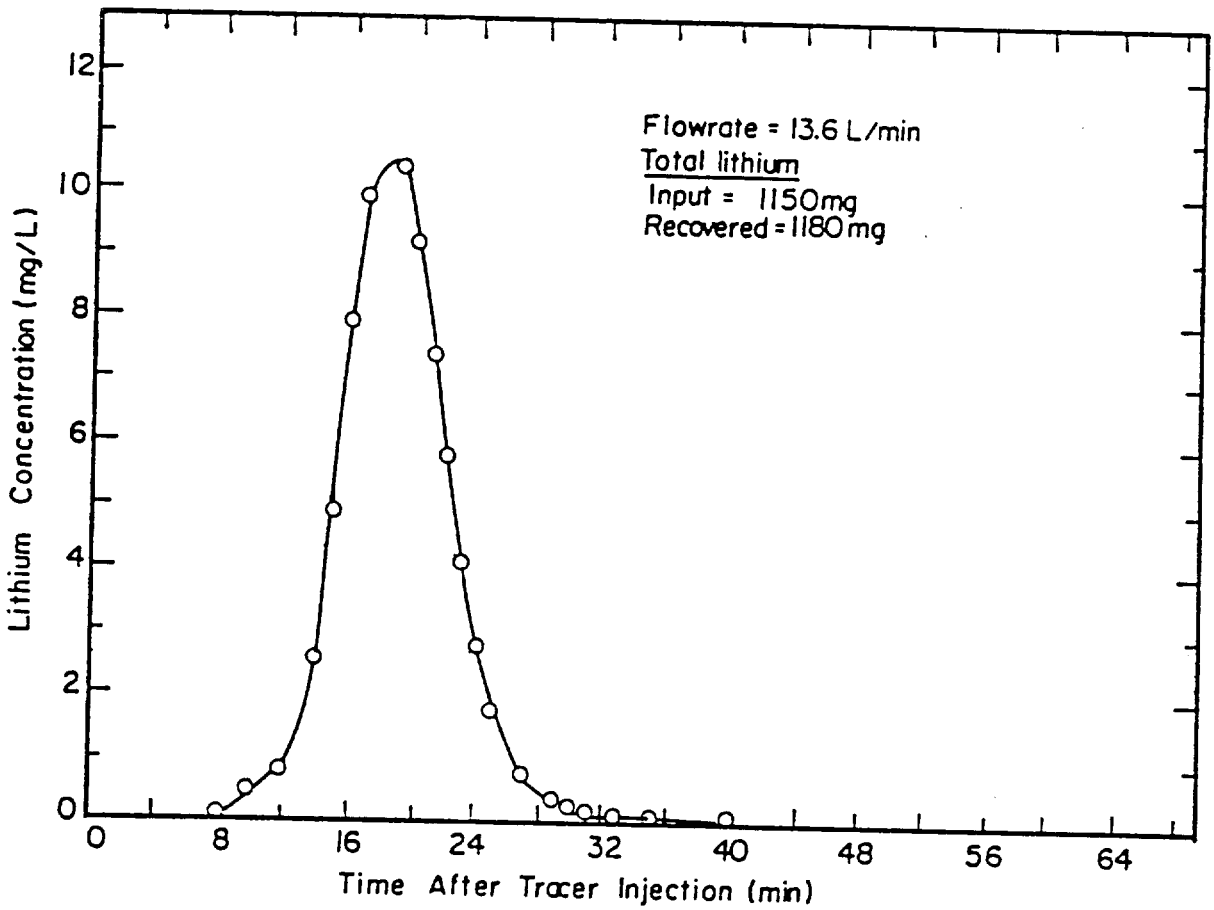


Figure 14. Measured effluent tracer concentration plotted as a function of the time elapsed after tracer injection for the baffled-box contactor (Figure 7).

be 10.4 min in the limestone and a total of 6.5 min in the nine sampling/baffle chambers (see Figure 7). The sum of these two quantities is approximately 17 min, a value which is in reasonable agreement with the mean residence time of 18 min determined using the tracer response data and Eq. 18. Also there was no evidence of significant short-circuiting or dead space.

## PIPE SECTION PROCEDURES

To evaluate metal corrosion prior to and following limestone treatment, pipe section leaching studies were conducted in both laboratory and field experiments. Most pipe section experiments were conducted with 1 m (3.3 ft) lengths of 1.27 cm (½ in.)inside diameter copper pipe. Copper pipe was amended with 2.54 cm (1 in.) of 50-50 percent lead-tin solder at both ends of a given section, to simulate Pb corrosion from Pb solder joints. A limited number of additional experiments were conducted with 1 m (3.3 ft) lengths of 1.59 cm (5/8 in.) lead and galvanized steel pipe.

The pipe cleaning procedure used was a modified version of the ASTM procedure. Pipe sections were soaked in 5% HCl for two minutes. These sections were then drained and rinsed with 0.1 N $NaHCO_3$ to neutralize any acidic solution adhering to the pipe. Finally, pipe sections were rinsed copiously with distilled deionized water.

During metal leaching studies, aliquots of solution were placed in pipe sections and the openings covered with parafilm. Solutions were equilibrated with pipe sections at room temperature (22°C), for a given period of time, generally 10 hours. Both pH and metal concentrations of leachate were measured after equilibrium.

## SAMPLING AND ANALYTICAL PROCEDURES

### General Procedures

The analytical methods used in this study are summarized in Table 10. Samples were collected in air-tight polyethylene containers for major solute and trace metal analysis, in a sterilized glass bottle for bacteriological analysis, and in biochemical oxygen demand bottles for oxygen analysis. Temperature was measured and dissolved oxygen samples were fixed in the field. Samples were transported in a cooler to the water quality laboratory at Syracuse

Table 10 Analytical Methods

| METHOD | PROCEDURE | REFERENCE |
|---|---|---|
| pH | potentiometrically with glass electrode | Standard Methods, 1975 |
| alkalinity | strong acid titration with Gran plot analysis | Gran, 1952 |
| $Ca^{2+}$, $Mg^{2+}$, $Na^{+}$, $K^{+}$ | atomic absorption spectrophotometry (AAS) | Slavin, 1968 |
| Al, Fe, Mn, Zn, Ca, Pb | filtration 0.4 μm polycarbonate filter, acidification (pH 1 with $HNO_3$ for 1 hr) analysis by AAS graphic furnace | Slavin, 1968 |
| $NO_3^-$, $Cl^-$ | ion chromatography | Small et al., 1975 |
| $SO_4^{2-}$ | ion chromotrography; turbidimetric method | Small et al., 1975; Standard Methods, 1975 |
| dissolved inorganic carbon (DIC) | syringe stripping of $CO_2$ and detection by gas chromatography | Stainton, 1973 |
| dissolved organic carbon (DOC) | filtration, ampoulation, persulfate oxidation, syringe stripping of $CO_2$ and detection by gas chromatography | Menzel & Vaccaro, 1964 |
| $NH_4^{+1}$ | phenate colorimetry, autoanalyzer | USEPA, 1983 |
| dissolved oxygen (D.O.) | Winkler titration | Standard Methods, 1985 |
| specific conductance | conductivity bridge | Standard Methods, 1985 |
| standard plate count | | Standard Methods, 1985 |
| coliform | membrane filter | Standard Methods, 1985 |
| turbidity | nephelometry | Standard Methods, 1985 |
| temperature | thermometer | |

University where they were measured for pH, alkalinity, specific conductance, dissolved inorganic carbon, dissolved oxygen, turbidity, coliform and standard plate count, and ampulated for the analysis of dissolved organic carbon within 8 hours of collection. Samples were stored at 4°C and analysis were completed within one week of collection.

Laboratory Contactors

Samples were collected starting at the top sampling point of the column and moving down the column using all the sampling ports provided. Samples were withdrawn by gravity flow and collected in 500 mL polyethylene bottles. To minimize $CO_2$ exchange, the bottles were completely filled and closed immediately. To minimize disturbance of the flow in the column during sampling, a period of time equal to twice the distance between two sampling ports divided by the interstitial flow velocity was allowed to elapse before the next sample was taken.

The column experiments were conducted at room temperature (15° - 22°C). To minimize microbial growth, the columns were initially rinsed with chlorinated water followed by deionized water. The clear acrylic column was covered with black plastic sheets to reduce exposure to light.

Field Contactors

Water samples were collected from the baffled box contactor and the housekeeping cottages connected to this unit for a period of 2.5 years. The sampling frequency was monthly except when weather conditions restricted access. Samples were also collected from the spring and cottages on the eastern side of the resort. This program included sampling at the cottage with the Culligan unit. A more frequent, sampling schedule was employed when the wound fiberglass unit was installed in Bay Side Cottage to treat Big Moose Lake water during January - April, 1984.

Two types of tap water samples were collected in the field, a flowing grab sample taken when the faucet was first opened and a grab sample obtained after 3 minutes of continuous flow.

Quality Assurance/Quality Control Information Data

An assessment of field data requires an understanding of the precision and accuracy associated with analytical determinations. In this study, both sampling and analytical precision were evaluated. Triplicate samples were

collected for analysis on a minimum of five percent of the total samples collected, and triplicate determinations were performed on a minimum of five percent of the samples collected. A summary of the range and coefficient of variation from the triplicate sampling (an estimate of sampling and analytical precision) program for a variety of water chemistry parameters is provided in Table 11. Moreover, we periodically performed a 4 by 4 analysis in which four samples were collected and split four ways. The resulting 16 solutions were analyzed for major solutes. By a two-way analysis of variance, (Barr et al. 1976) the sampling and analytical precision were evaluated (Table 12).

To evaluate analytical accuracy we performed charge balances, conductivity checks, and alkalinity checks (Figure 15). Also we periodically evaluated blind samples obtained from the USEPA Municipal Environmental Research Laboratory at Cincinnati, Ohio; the USGS Standard Reference Water Sample Program, Denver, Colorado; and the USEPA Long-Term Monitoring Program through Radian Inc. Results of some blind audit samples obtained from the USEPA Municipal Environmental Research Laboratory are summarized in Table 13. Generally the analyses of audit samples from this program were in agreement with reported values. However, this audit program was not designed to evaluate analytical accuracy of the low concentration ranges generally observed in dilute waters. A more reasonable depiction of the accuracy of our analytical methods is available through the analysis of dilute audit samples from the USEPA Long-Term Monitoring Program conducted in May 1985 (Table 14). Although the percent differences between the theoretical and values obtained by Radian Compared to the values reported by Syracuse University were high for some determinations, the actual magnitude of these discrepancies were generally low. These relatively high percent differences may be attributed to the low solute concentrations in this particular sample. Note some decrease in pH and increase in DIC is evident between determinations made by Radian and analyses conducted by Syracuse University, however ANC values were similar. These trends suggest that when this synthetic sample was made-up it was undersaturated with respect to the solubility of atmospheric $CO_2$. Over storage time, $CO_2$ equilibration evidently served to depress pH values while increasing DIC concentrations. Some discrepancy in DOC concentrations are also evident, however, given that the source of this synthetic DOC is unknown, this trend is difficult to explain.

TABLE 11
Summary of Sampling and Analytical Precision from Sample Triplicate Program

| Parameter | Range of Mean | Range of Standard Deviation | Range of Coefficient of Variation |
|---|---|---|---|
| pH | 6.01 - 7.68 | 0.006 - 0.231 | 0.079 - 3.0 |
| alkalinity (mg $CaCO_3 \cdot L^{-1}$) | 7.7 - 34 | 0.29 - 1.0 | 0.85 - 3.6 |
| Sp. Cond. ($\mu mho \cdot cm^{-1}$) | 50 - 107 | 0.12 - 6.2 | 0.12 - 5.8 |
| DIC (mg $C \cdot L^{-1}$) | 4.9 - 7.7 | 0.06 - 0.60 | 0.84 - 9.1 |
| DOC (mg $C \cdot L^{-1}$) | 0.76 - 2.3 | 0 - 0.30 | 5.0 - 10 |
| Turbidity (NTU) | 0.31 - 0.53 | 0.035 - 0.10 | 11 - 20 |
| DO (mg $O_2 \cdot L^{-1}$) | 7.0 - 7.3 | 0.1 - 0.5 | 1.4 - 7.6 |
| Standard Plate Count (#·100 $mL^{-1}$) | 3.7 - 195 | 1.1 - 36 | 20 - 31 |
| Total Coliform (#·100 $mL^{-1}$) | 0 - 64 | 0 - 16 | 0 - 25 |
| Ca (mg $Ca \cdot L^{-1}$) | 5.3 - 12.2 | 0.08 - 0.67 | 0.94 - 5.5 |
| Mg (mg $Mg \cdot L^{-1}$) | 0.65 - 0.89 | 0 - 0.016 | 0 - 1.8 |
| Na (mg $Na \cdot L^{-1}$) | 2.4 - 7.2 | 0.012 - 1.36 | 0.46 - 19 |
| K (mg $K \cdot L^{-1}$) | 0.66 - 2.6 | 0 - 0.25 | 0 - 9.4 |
| $SO_4$ (mg $SO_4 \cdot L^{-1}$) | 4.0 - 4.3 | 0.21 - 0.40 | 5 - 10 |
| Al ($\mu g$ $Al \cdot L^{-1}$) | 0 - 33 | 3 - 16 | 29 - 48 |
| Cu ($\mu g$ $Ca \cdot L^{-1}$) | 0 - 1 | 0 - 2 | 0 - 43 |
| Pb ($\mu g$ $Pb \cdot L^{-1}$) | 0 - 123 | 0 - 7 | 0 - 55 |
| Zn ($\mu g$ Zn·L-1) | 13 - 42 | 20 - 32 | 60 - 76 |

TABLE 12 Estimates of sample collection and analytical precision from 4 x 4 analysis for Big Moose Lake

| Parameter | Sampling Precision | | Analytical Precision | |
|---|---|---|---|---|
| | Std. Dev. | C.V. | Std. Dev. | C.V. |
| field pH | 0.020 | 0.39 | 0.0088 | 0.17 |
| air equilibrated pH | 0.028 | 0.54 | 0.012 | 0.23 |
| ANC ($\mu eq \cdot L^{-1}$) | 2.6 | 44 | 5.1 | 86 |
| Spec. Cond($\mu mho \cdot cm^{-1}$) | 2.1 | 5.9 | 0.3 | 0.84 |
| Ca($\mu mol \cdot L^{-1}$) | 0.49 | 1.0 | 0.36 | 0.78 |
| Mg($\mu mol \cdot L^{-1}$) | 0.02 | 1.5 | 0.003 | 0.79 |
| Na($\mu mol \cdot L^{-1}$) | 0.77 | 2.8 | 0.14 | 0.52 |
| K($\mu mol \cdot L^{-1}$) | 0.34 | 3.2 | 0.13 | 1.2 |
| monomeric Al ($\mu mol \cdot L^{-1}$) | 0.40 | 9.6 | 0.19 | 4.9 |
| $SO_4^{2-}$($\mu mol \cdot L^{-1}$) | 2.9 | 4.3 | 0.61 | 0.90 |
| $NO_3^-$($\mu mol \cdot L^{-1}$) | 1.3 | 6.9 | 0.76 | 4.0 |
| $Cl^-$($mol \cdot L^{-1}$) | 1.6 | 19 | 0.83 | 9.5 |
| $H_2SO_4$($\mu mol \cdot L^{-1}$) | 5.1 | 6.9 | 1.7 | 2.3 |
| DOC($\mu mol \cdot L^{-1}$) | 54 | 14 | 21 | 5.4 |
| DIC($\mu mol \cdot L^{-1}$) | 1.6 | 6.8 | 1.4 | 1.9 |
| Free F($\mu mol \cdot L^{-1}$) | 0.018 | 3.4 | 0.0095 | 1.8 |
| Total F($\mu mol \cdot L^{-1}$) | 0.14 | 3.2 | 0.059 | 1.4 |

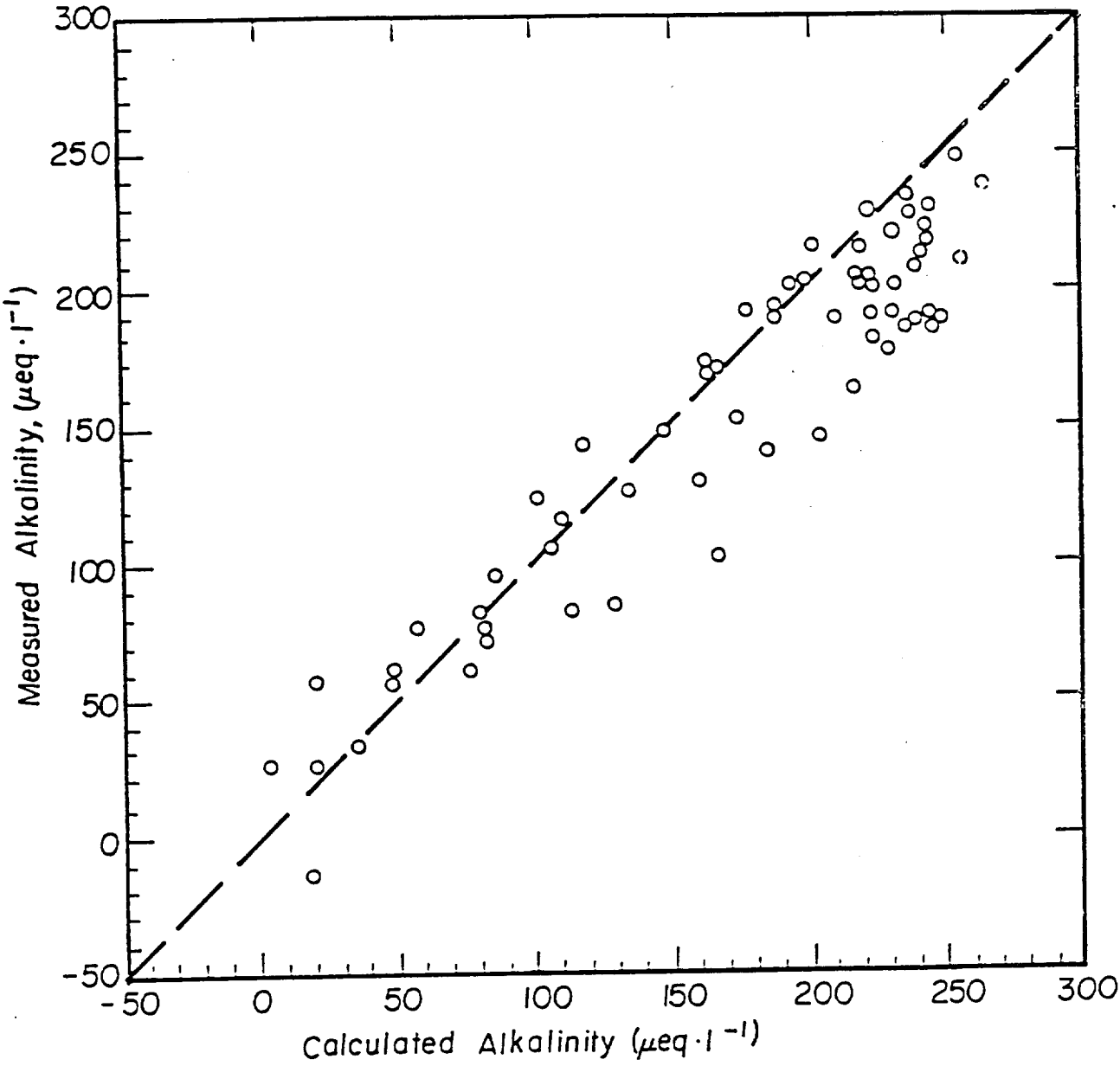


Figure 15. Measured and calculated alkalinity for field measurements. The measured dissolved inorganic carbon concentration and pH were used to determine the "calculated" alkalinity.

TABLE 13

Summary of Blind Sample Analysis Obtained from USEPA Municipal Environmental Research Laboratory

| Date | Parameter | True Value | Measured Value | % Difference |
|---|---|---|---|---|
| 7/1/82 | Turbidity (NTU) | 1.35 | 1.30 | 6.7 |
| | Turbidity (NTU) | 5.50 | 5.35 | 2.7 |
| | $NO_3^-$(mg $N \cdot L^{-1}$) | 0.42 | 0.42 | 0 |
| | $NO_3^-$(mg $N \cdot L^{-1}$) | 7.3 | 7.3 | 0 |
| | $F^-$(mg $F \cdot L^{-1}$) | 0.12 | 0.12 | 0 |
| | $F^-$(mg $F \cdot L^{-1}$) | 1.1 | 1.1 | 0 |
| 10/1/82 | Pb(µg $Pb \cdot L^{-1}$) | 25 | 25 | 0 |
| | Zn(µg $Zn \cdot L^{-1}$) | 15 | 16 | -6.7 |
| | Al(µg $Al \cdot L^{-1}$) | 78 | 78 | 0 |
| | Mn(µg $Mn \cdot L^{-1}$) | 15 | 16 | -6.7 |
| | Mn(µg $Mn \cdot L^{-1}$) | 75 | 68 | 9.3 |
| | Fe(µg $Fe \cdot L^{-1}$) | 80 | 81 | -1.2 |
| | Fe(µg $Fe \cdot L^{-1}$) | 900 | 890 | 1.1 |
| 7/5/83 | Turbidity (NTU) | 5.9 | 5.6 | 5.1 |
| | Turbidity (NTU) | 0.42 | 0.31 | 26 |
| | Pb(µg $Pb \cdot L^{-1}$) | 22 | 21 | 4.5 |
| | Pb(µg $Pb \cdot L^{-1}$) | 56 | 43 | 23 |
| | Cd(µg $Cd \cdot L^{-1}$) | 1.2 | 2.3 | -92 |
| | Cd(µg $Cd \cdot L^{-1}$) | 22 | 22 | 0 |

TABLE 13 (con't)

| Date | Parameter | True Value | Measured Value | % Difference |
|---|---|---|---|---|
| 12/14/83 | pH | 6.87 | 6.84 | |
| | pH | 8.60 | 8.45 | |
| | Sp. Cond($\mu$mho$\cdot$cm$^{-1}$) | 215 | 235 | -9.3 |
| | Sp. Cond($\mu$mho$\cdot$cm$^{-1}$) | 616 | 685 | -11 |
| | Ca(mg Ca$\cdot$L$^{-1}$) | 4.8 | 4.8 | 0 |
| | Ca(mg Ca$\cdot$L$^{-1}$) | 32 | 32 | 0 |
| | Mg(mg Mg$\cdot$L$^{-1}$) | 1.26 | 1.20 | 4.7 |
| | Mg(mg Mg$\cdot$L$^{-1}$) | 9.46 | 9.41 | 0.5 |
| | Na(mg Na$\cdot$L$^{-1}$) | 33.3 | 35.6 | -6.9 |
| | Na(mg Na$\cdot$L$^{-1}$) | 68.5 | 77 | 1.3 |
| | K(mg K$\cdot$L$^{-1}$) | 0.62 | 1.52 | -145 |
| | K(mg K$\cdot$L$^{-1}$) | 12.3 | 17.0 | -38 |
| | Cu($\mu$g Ca$\cdot$L$^{-1}$) | 78.0 | 73.0 | 6.4 |
| | Cu($\mu$g Cu$\cdot$L$^{-1}$) | 5.20 | 5.80 | -11 |
| | Pb($\mu$g Pb$\cdot$L$^{-1}$) | 158 | 170 | -7.5 |
| | Pb($\mu$g Pb$\cdot$L$^{-1}$) | 11.7 | 30 | -156 |
| 1/13/84 | Turbidity (NTU) | 6.0 | 6.8 | -13 |
| | Turbidity (NTU) | 0.7 | 1.2 | -71 |
| | Pb($\mu$g Pb$\cdot$L$^{-1}$) | 30 | 45 | -50 |
| | Pb($\mu$g Pb$\cdot$L$^{-1}$) | 90.1 | 94 | -4.3 |
| 7/16/84 | Cd($\mu$g Cd$\cdot$L$^{-1}$) | 2.1 | 1.8 | 14 |
| | Cd($\mu$Cd$\cdot$L$^{-1}$) | 10.8 | 8.8 | 18 |
| | Pb($\mu$g Pb$\cdot$L$^{-1}$) | 37.6 | 29 | 23 |
| | Pb($\mu$g Pb$\cdot$L$^{-1}$) | 105 | 86 | 18 |

[1]%Difference = (True Value - Reported Value)/(True Value) x 100

TABLE 14 Summary of USEPA Corvallis Environmental Research Laboratory Blind Audit Analysis.
All values in $\mu eq \cdot L^{-1}$ except where indicated.

| Parameter | Theoretical | Radian Value | Syracuse Univ. | | %Difference Theoretical | | Radian | |
|---|---|---|---|---|---|---|---|---|
| | | | 839 | 840 | 839 | 840 | 839 | 840 |
| pH | ------ | 7.31 | 6.67 | 6.96 | --- | --- | --- | --- |
| alkalinity | ------ | 108 | 113 | 110 | --- | --- | --- | --- |
| $SO_4^{2-}$ | 48 | 49 | 44 | 45 | --- | --- | 4 | 2 |
| $NO_3^-$ | 7.4 | 7.9 | 7.0 | 8.2 | -9 | -7 | -11 | -9 |
| $F^-$ | 2.2 | 2.2 | 2.6 | 2.4 | 15 | 8 | 15 | 8 |
| $Ca^{2+}$ | 9.8 | 11.1 | 13 | 12 | 25 | 18 | 15 | 8 |
| $Mg^{2+}$ | 37 | 35 | 39 | 39 | 5 | 5 | 10 | 10 |
| $Na^+$ | 121 | 117 | 118 | 109 | -3 | -11 | 1 | -7 |
| $K^+$ | 5.2 | 4.8 | 5 | 4 | -4 | -30 | 4 | -10 |
| $NH_4^+$ | 9.3 | 8.3 | 12.1 | 10.7 | 23 | 13 | 31 | 22 |
| DOC($\mu mol \cdot L^{-1}$) | 83 | 98 | 140 | 152 | 41 | 45 | 30 | 36 |
| DIC($\mu mol \cdot L^{-1}$) | ------ | 98 | 138 | 138 | --- | --- | 29 | 29 |
| $SiO_2$($\mu mol \cdot L^{-1}$) | 18 | 18 | 20 | 20 | 10 | 10 | 10 | 10 |
| Sp. Cond. ($\mu mol \cdot cm^{-1}$) | ------ | 17.3 | 20 | 20 | --- | --- | 6 | 6 |
| Cal. Sp. Cond. | ------ | 18.6 | 19.3 | 18.5 | | | | |
| sum of cations | ------ | 176 | 187 | 175 | | | | |
| sum of anions | ------ | 177 | 180 | 179 | | | | |
| Cal. $HCO_3^-$ | ------ | 90 | 98 | 99 | | | | |

Samples were routinely split with other researchers that analyze low ionic strength solutions. Analytical checks on dilute solutions have been made with investigators from Cornell University, McMaster University, University of Virginia, University of California at Los Angeles, the Insitute of Ecosystem Studies Cary Arboretum, and Rensselaer Polytechnic Institute.

## COMPUTATIVE ANALYSIS

Thermodynamic calculations involving trace metal solubility were conducted with a modified version of the chemical equilibrium model MINEQL (Westall et al., 1976). Calculations were corrected for the effects of ionic strength using the Davies equations (Stumm and Morgan, 1981) and temperature. The solubility and complexation constants used in our analysis are summarized in Tables 15 and 16, respectively. The results obtained from chemical equilibrium calculations are highly dependent on the thermochemical data used. Data analysis is complicated by inconsistencies in the literature. In this regard, we conducted a thorough review to evaluate if there was consensus among researchers in the use of thermodynamic data relevent to our study (Tables 15 and 16). The results of this literature search suggest that generally there is consensus in the use of thermochemical data. However, some inconsistencies were evident in trace metal reactions.

There is considerable uncertainty in the stability constant for $Cu(OH)_2(aq)$ (Vacenta, 1976). This uncertainty is significant because predictions of total Cu in the neutral pH range are very sensitive to this stability constant. The stability constant for $Cu(OH)_2(aq)$ was evaluated potentiometrically by Quintin (1937), obtaining a value of $\log^* \beta_2 = -13.7$; while Spivakovski and Makouskaya (1968) used a precipitation method to obtain $\log^* \beta_2 = 13.2$. However, Mesmer and Baes (1974) estimated $\log^* \beta_2 = -17.3$, almost four orders of magnitude lower than previous estimates. Vacenta (1976) noted the magnitude and significance in this discrepancy. She evaluated the $Cu(OH)_2(aq)$ stability constant potentiometrically with a Cu ion selective electrode and obtained results consistent with $\log^* \beta_2 = -13.7$. Therefore we followed her lead and used this value in our study.

Another perplexing inconsistency in thermodynamic data involves the solubility of $Pb(OH)_2(s)$. Wagman et al. (1968) reported a value log* Kso

TABLE 15 Equilibrium Constants at 25°C for the Solids Considered in the MINEQL Calculations.

| | REACTIONS | | log K | REFERENCE |
|---|---|---|---|---|
| 1. | $Cu(OH)_{2(s)} + 2H^+$ | $Cu^{+2} + 2H_2O$ | - 8.64 | Baes and Mesmer 1976 |
| 2. | $CuCO_{3(s)}$ | $Cu^{+2} + CO_3$-2 | - 9.63 | Smith and Martell 1976 |
| 3. | $Cu_2(OH)_2CO_3 + 3H^+$ | $2Cu^{+2} + HCO_3^- + 2H_2O$ | 5.15 | Baes and Mesmer 1976 |
| 4. | $Cu_3(OH)_2(CO_3)_2 + 4H^+$ | $3Cu^{+2} + 2HCO_3^- + 2H_2O$ | 3.75 | Baes and Mesmer 1976 |
| 5. | $CuSO_4$ | $Cu^{+2} + SO_4^{-2}$ | 3.01 | Wagman et al 1969 |
| 6. | $Pb(OH_{2(s)} + 2H^+$ | $Pb^{+2} + 2H_2O$ | 8.15-13.07 | Wagman et al 1969<br>Topelman 129 |
| 7. | $PbCO_{3(s)}$ | $Pb^{+2} + CO_3^{-2}$ | -13.13 | Hem 1976 |
| 8. | $Pb_3(CO_3)_2(OH)_{2(s)} + 2H^+$ | $3Pb^{+2} + 2CO_3^{-2}$ | -17.46 | Sillen and Martell 1964 |
| 9. | $PbSO_{4(s)}$ | $Pb^{+2} + SO_4^{-2}$ | - 7.79 | Smith and Martell 1976 |
| 10. | $Zn(OH)_{2(s)} + 2H^+$ | $Zn^{+2} + 2H_2O$ | 12.45 | Baes and mesmer 1976 |
| 11. | $ZnCO_{3(s)}$ | $Zn^{+2} + CO_3^{-2}$ | -10.00 | Smith and Martell 1976 |
| 12. | $Zn_5(OH)_6(CO_3)_{2(s)} + 6H^=$ | $5Zn^{+2} + 2CO_3^{-2} + 6H_2O$ | 9.65 | Sillen and Martell 1964 |
| 13. | $ZnSO_{4(s)}$ | $Zn^{+2} + SO_4^{-2}$ | 3.01 | Wagmann et al 1969 |

TABLE 16 REACTIONS AND EQUILIBRIUM CONSTANTS AT 25°C FOR THE AQUEOUS COMPLEXES CONSIDERED IN THE MINEQL CALCULATIONS

| | REACTIONS | | log K (Ball et al., 1980) | | |
|---|---|---|---|---|---|
| | | | Pb | Cu | Zn |
| 1. | $M^{+2} + H_2O$ | $\longrightarrow MOH^+ + H^+$ | - 7.71 | - 8.00 | - 8.96 |
| 2. | $M^{+2} + 2H_2O$ | $\longrightarrow M(OH)_2^0 + 2H^+$ | -17.12 | -13.68 | -16.90 |
| 3. | $M^{+2} + 3H_2O$ | $\longrightarrow M(OH)_3 + 3H^+$ | -28.06 | -26.90 | -28.40 |
| 4. | $M^{+2} + 4H_2O$ | $\longrightarrow M(OH)_2^{-2} + 4H^+$ | -39.70 | -39.60 | -41.20 |
| 5. | $2M^{+2} + H_2O$ | $\longrightarrow M_2OH^{+3} + H^+$ | - 6.36 | ------ | - 9.00 |
| 6. | $2M^{+2} + 2H_2O$ | $\longrightarrow M_2(OH)_2 + 2H^+$ | ------ | -10.36 | ------ |
| 7. | $3M^{+2} + 4H_2O$ | $\longrightarrow M_3(OJ)_4^{+2} + 2H^+$ | -23.88 | -22.05 | ------ |
| 8. | $4M^{+2} + 4H_2O$ | $\longrightarrow M_4(OH)_8^{+4} + 4H^+$ | -20.88 | ------ | ------ |
| 9. | $6M^{+2} + 8H_2O$ | $\longrightarrow M_6(OH)_8^{+4}$ | -43.61 | ------ | ------ |
| 10. | $M^{+2} + CO_3^{-2} + H^+$ | $\longrightarrow MHCO_3^+$ | ------ | 13.03 | 12.43 |
| 11. | $M^{+2} + CO_3^{-2}$ | $\longrightarrow MCO_3^0$ | 7.24 | 6.73 | 5.30 |
| 12. | $M^{+2} + 2CO_3^{-2}$ | $\longrightarrow M(CO_3)_2^{-2}$ | 10.64 | 9.83 | 9.63 |
| 13. | $M^{+2} + Cl^-$ | $\longrightarrow MCL^+$ | 1.60 | 0.43 | 0.43 |
| 14. | $M^{+2} + 2Cl^-$ | $\longrightarrow MCl_2^0$ | 1.80 | 0.16 | 0.45 |
| 15. | $M^{+2} + 3Cl^-$ | $\longrightarrow MCl_3^-$ | 1.70 | - 2.29 | 0.30 |
| 16. | $M^{+2} + 4Cl^-$ | $\longrightarrow MCl_4^-$ | ------ | - 4.59 | 0.20 |
| 17. | $M^{+2} + SO_4^{-2}$ | $\longrightarrow MSO_4^0$ | 2.75 | 2.31 | 2.37 |

= 8.15. This value has been used throughout the literature in studies of Pb chemistry (e.g. Hem and Durum, 1973; Ball et al., 1980; Faust and Aly, 1981). Topelmann (1929) obtained log* Kso = 13.07 for "freshly precipitated" $Pb(OH)_2$. This latter value has been cited by Feithnecht and Schindler (1963), and ultimately used by Patterson et al. (1977), and Schock (1980, 1984) in studies of Pb corrosion in water distribution systems. Schock (1980) indicated that the discrepancy between the two solubility values represents the difference between "fresh" and "aged" precipitates. However given the magnitude of this discrepancy (5 orders of magnitude), it is doubtful that crystallinity of the precipitate explains the variation. Note that the value obtained by Wagman et al. (1968) was calculated, not experimental. While Topelmann's (1929) work was experimental the magnitude of experimental error in his study in unclear. Therefore one value is not obviously superior to the others; in fact the validity of both values could be challenged. The solubility of $Pb(OH)_2$ is a classic example of thermochemical data finding its way in the literature and gaining acceptance over years of use without the benefit of a critical review. Clearly if we are to improve our understanding of Pb corrosion, better information on the solubility of $Pb(OH)_2$ is desperately needed.

In this study statistical analysis was facilitated by the use of the Statistical Analysis System (SAS; Barr et al., 1976).